European Journal of Radiology 112 (2019) 106–111

Contents lists available at ScienceDirect

European Journal of Radiology

journal homepage: www.elsevier.com/locate/ejrad

Detection of occult neoplastic infiltration in the corpus callosum and prediction of overall survival in patients with glioblastoma using diffusion tensor imaging

Suyash Mohan[a,*], Sumei Wang[a], Gokcen Coban[b], Feride Kural[c], Sanjeev Chawla[a], Donald M. O'Rourke[d], Harish Poptani[a,e]

[a] Department of Radiology, Division of Neuroradiology, Perelman School of Medicine at the University of Pennsylvania, Philadelphia, PA, USA
[b] Department of Radiology, Hacettepe University Medical School, Ankara, Turkey
[c] Department of Radiology, Baskent University School of Medicine, Ankara, Turkey
[d] Department of Neurosurgery, Perelman School of Medicine at the University of Pennsylvania, Philadelphia, PA, USA
[e] Department of Cellular and Molecular Physiology, University of Liverpool, Liverpool, UK

ARTICLE INFO

Keywords:
Glioblastoma
Diffusion tensor imaging
Corpus callosum
Prognosis
Survival

ABSTRACT

Objective: Corpus callosum (CC) involvement is a poor prognostic factor in patients with glioblastoma (GBM). The purpose of this study was to determine whether diffusion tensor imaging (DTI) can quantify occult tumor infiltration in the CC and predict the overall survival in GBM patients.

Methods: Forty-eight patients with pathologically proven GBM and 17 normal subjects were included in this retrospective study. Patients were divided into four groups based on CC invasion and overall survival: long survivors without CC invasion; short survivors without CC invasion; long survivors with CC invasion; short survivors with CC invasion. All patients underwent DTI at 3T MRI scanner. Fractional anisotropy (FA) and mean diffusivity (MD) values were measured from genu, mid-body, and splenium of the CC. The mean values of these parameters were compared between different groups and Kaplan Meier curves were used for prediction of overall survival.

Results: Patients with short survival and CC invasion had the lowest FA values (0.64 ± 0.05) from the CC compared with other groups ($p < 0.05$). Receiver operator characteristic curve (ROC) analysis indicated that a FA cutoff value of 0.70 was the best predictor for overall survival with an area under the curve (AUC) of 0.77, sensitivity 1, specificity 0.59. Kaplan-Meier survival curves demonstrated that the mean survival time was significantly longer for patients with high FA (> 0.70) compared with those with low FA (< 0.70) ($p < 0.001$).

Conclusions: FA values from the CC can quantify occult tumor infiltration and serve as a sensitive prognostic marker for prediction of overall survival in GBM patients.

1. Introduction

Glioblastoma (GBM) is the most malignant brain tumor and accounts for 70% of all primary brain tumors in adults. Despite intensive multimodal treatment including maximal surgical resection and chemoradiation, the prognosis of newly diagnosed GBM is poor and median overall survival (OS) is less than 15 months with a 2-year survival rate of 26–33% [1,2]. GBM is an extremely invasive tumor, characterized by the absence of discrete boundaries on imaging as well as on histology. Histopathological studies have reported malignant cells in normal appearing white matter not only remote from the primary neoplasm but also in the contralateral cerebral hemisphere [3–5]. The occult spread of malignant GBM cells into normal brain is one of the major determinants for the poor prognosis of this aggressive neoplasm [3,6,7]. Corpus callosum (CC), the largest commissural tract in the brain, may provide an avenue for neoplastic cells to infiltrate into the contralateral

Abbreviations: GBM, glioblastoma; CC, corpus callosum; OS, overall survival; DTI, diffusion tensor imaging; MD, mean diffusivity; FA, fractional anisotropy; ROI, region of interest; HIPAA, Health Insurance Portability and Accountability Act; GRAPPA, generalized autocalibrating partially parallel acquisition; AUC, area under the curve; ROC, receiver operating characteristic

* Corresponding author at: Department of Radiology, Division of Neuroradiology, Perelman School of Medicine at the University of Pennsylvania, 3400 Spruce St., Philadelphia, PA, 19104, USA.
E-mail address: suyash.mohan@uphs.upenn.edu (S. Mohan).

https://doi.org/10.1016/j.ejrad.2019.01.015
Received 24 July 2018; Received in revised form 29 November 2018; Accepted 14 January 2019

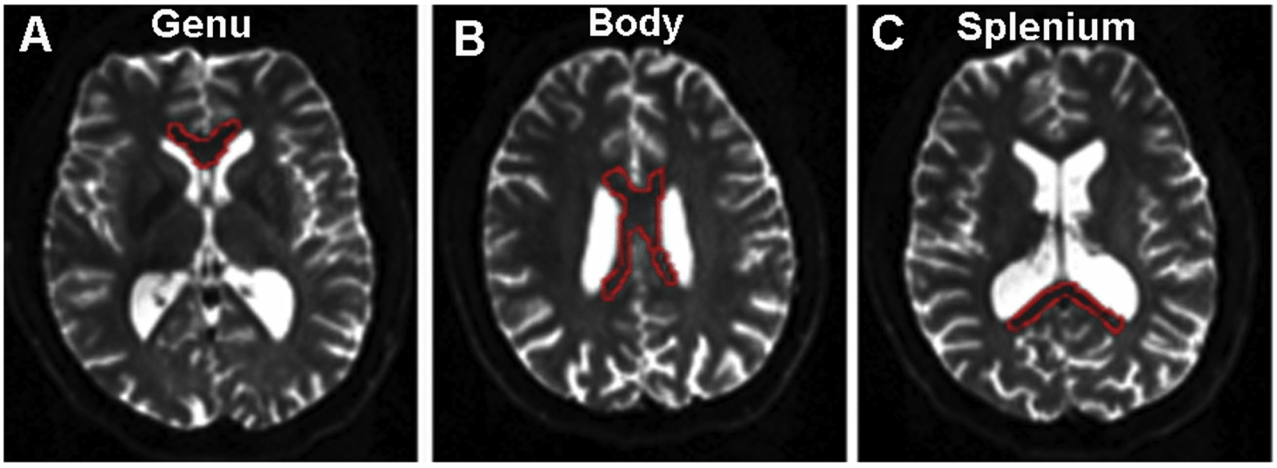

Fig. 1. Regions of interest on axial T2 weighted images (red) at the level of genu (A), mid-body (B) and splenium (C) of corpus callosum.

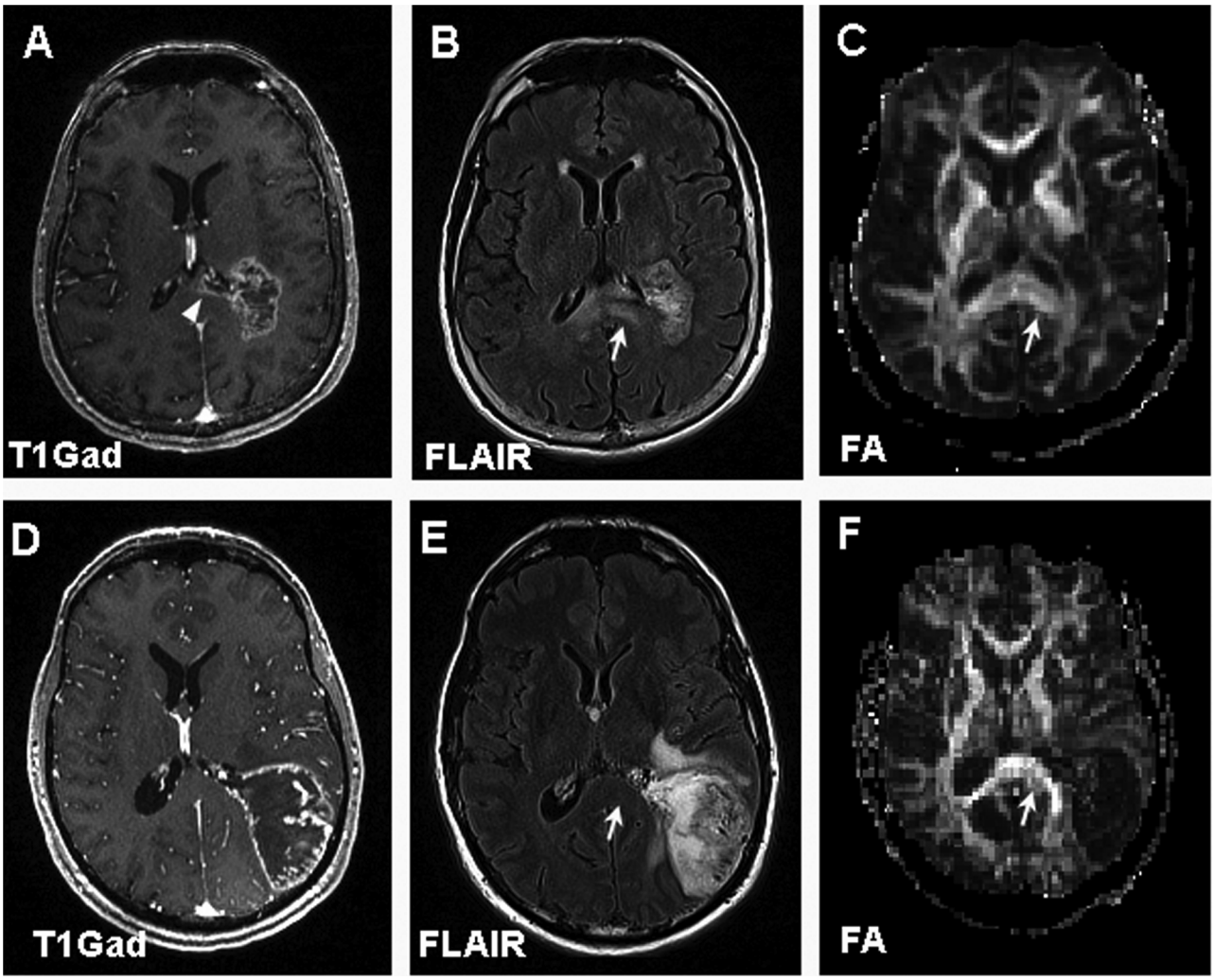

Fig. 2. MR images of 70-year-old female glioblastoma patients with corpus callosum invasion (top panel) (A, B, C) and 53-year-old male glioblastoma patients without corpus callosum invasion (bottom panel) (D, E, F). Axial contrast-enhanced T1 weighted images (A, D) demonstrate extension of enhancing tumor into the splenium of CC in (A) (arrowhead), with normal appearing CC in (D). Axial FLAIR images (B, E) demonstrate corresponding expansile infiltrative FLAIR signal abnormality in the splenium of corpus callosum (arrow) in (B), whereas the CC seems uninvolved in E (arrow). Lower FA from the splenium of corpus callosum is noticed in FA map (C, arrow) for the patient with short survival than the one with longer overall survival (F, arrow).

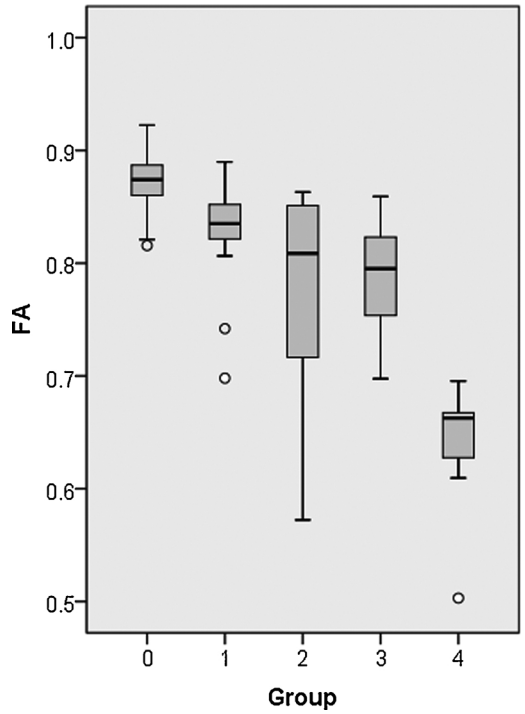

Fig. 3. Box plot of FA from the corpus callosum (CC) in GBM patients with short and long survival. The solid line inside the box represents the median value, while the edges represent the 25th and 75th percentiles. Straight line (bars) on each box indicates the range of data distribution. Circle represent outliers (values more than 1.5 box length from the 75th/25th percentile).
0. Control group.
1. Long survivors without CC invasion.
2. Short survivors without CC invasion.
3. Long survivors with CC invasion.
4. Short survivors with CC invasion.
Comparison between group 1 and 2 ($p = 0.14$), group 2 and 3 ($p = 0.95$) didn't reach significant difference. There were significant differences between all other groups ($p < 0.05$) (Table 1)

Table 1
P values of pairwise comparison between different groups using Mann-Whitney *U* test.

Group	0	1	2	3	4
0		0.004*	0.000*	0.000*	0.000*
1	0.004*		0.140	0.020	0.000*
2	0.000*	0.140		0.950	0.006*
3	0.000*	0.020	0.950		0.000*
4	0.000*	0.000*	0.006*	0.000*	

0. Control group.
1. Long survivors without CC invasion.
2. Short survivors without CC invasion.
3. Long survivors with CC invasion.
4. Short survivors with CC invasion.
* Indicates significant difference after bonferroni correction ($p < 0.01$).

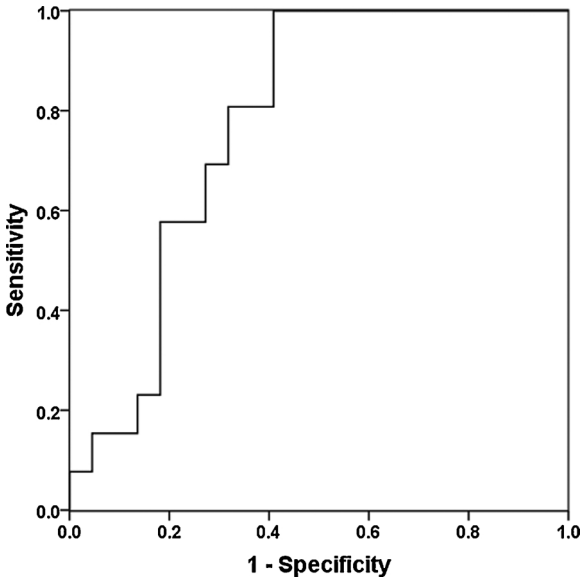

Fig. 4. Receiver operative characteristic (ROC) curve demonstrates that FA value from the corpus callosum is the best predictor for overall survival with the area under the curve (AUC) of 0.77, sensitivity 1, specificity 0.59 using a cutoff value of 0.70.

hemisphere [4]. The extent of CC infiltration could probably be used as a surrogate of aggressiveness and invasiveness of the tumor, potentially providing useful prognostic information [3,8,9].

While conventional MR imaging can demonstrate the size, shape, and location of the tumor, it is limited in delineating the extent of microscopic tumor infiltration. Diffusion tensor imaging (DTI) can identify disruption of the white matter microstructure and can thus be utilized as a tool for detection of occult neoplastic invasion in normal appearing areas of brain on conventional MR imaging [7,10]. Changes in diffusion properties can be assessed by the measurement of mean diffusivity (MD) and fractional anisotropy (FA). Previously published studies have reported reduced FA in the normal appearing CC, indicating that DTI can potentially detect tumor infiltration in GBM patients [10,11]. Studies involving animal models of brain tumors have also confirmed that DTI can detect glioma cell migration/invasion that precedes formation of tumor mass [12].

In this retrospective study, we applied regions of interest (ROI) analysis and measured FA and MD from the genu, splenium and body of CC. We hypothesized that these DTI metrics can quantify tumor infiltration in the CC and predict OS in GBM patients.

2. Materials and Methods

2.1. Patients

The study was approved by the institutional review board and was compliant with the Health Insurance Portability and Accountability Act (HIPAA). Forty-eight patients (30 men and 18 women; mean age 62.40 ± 12.5 years; age range, 22–89 years) with pathologically proven GBM were retrospectively identified from our institution database from June 2006 to December 2013. The primary inclusion criteria for the enrollment of patients in the present study were: (a) gross total resection of their neoplasms so that extent of resection (fraction of residual tumor) may not be a confounding factor in the survival analysis (b) all neoplastic lesions demonstrated contrast enhancement on post-contrast T1 weighted images (c) availability of good quality DTI data. All of these patients underwent gross total resection of the tumor followed by standard radiation therapy and temozolomide chemotherapy and 8 patients received bevacizumab therapies. Karnofsky performance status (KPS) after the surgery ranged from 20 to 80%. In addition, 17 healthy subjects were included as normal controls (4 men, 13 women, mean age 60.35 ± 13.5 years, age range 25–72 years).

The survival time of all the patients was recorded from the date of initial diagnosis to the date of death. The median OS time from our cohort of 48 patients was 14.0 months (range 1–58 months), which was used as a cut-off to separate the patients into two groups. Patients demonstrating OS duration of greater than 14 months were defined as *long-term survivors* while patients who died in less than14 months were defined as *short-term survivors*

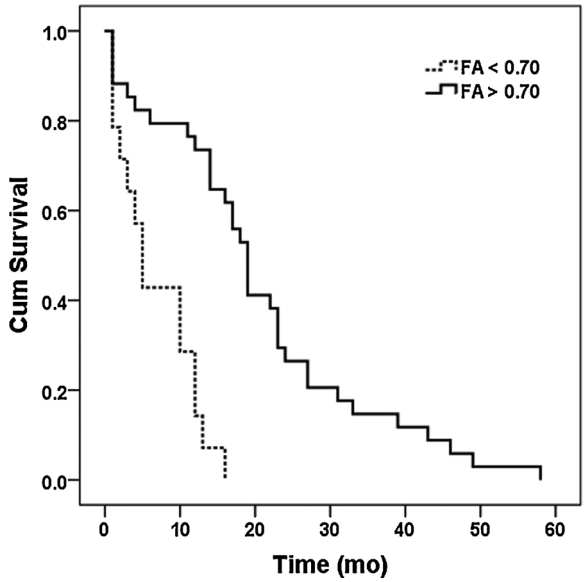

Fig. 5. Kaplan-Meier curves for patients with glioblastoma with low FA (< 0.70, dotted line) and high FA (> 0.70, solid line). Patients with high FA (> 0.70) had a mean survival time of 20.41 ± 14.31 months whereas patients with low FA (< 0.70) had a mean overall survival time of 6.79 ± 5.19 months. There was a significant difference in patients with high FA and low FA ($p < 0.001$).

2.2. Data acquisition

MR imaging studies were performed on a Tim Trio 3T whole-body scanner (Siemens, Erlangen, Germany) by using a 12-channel phased array head coil. Routine diagnostic imaging sequences included axial T1 weighted 3D MPRAGE (TR/TE/TI 1760/3.1/950 ms, 192 × 256 matrix size, 1 mm section thickness) and axial FLAIR (TR/TE/ TI 9420/ 141/2500 ms, 3 mm section thickness). DTI data were acquired using a single-shot spin-echo EPI sequence with parallel imaging by using generalized autocalibrating partially parallel acquisition (GRAPPA) and an acceleration factor of 2. Diffusion weighting was applied in 30 isotropically distributed directions by using a b-value of 1000 s/mm^2, with a total acquisition time of 8 min. Other sequence parameters were as follows: TR/TE 5000/86 ms, NEX = 3, FOV = 22 × 22 cm^2, slice thickness = 3 mm, number of sections = 40. Post-contrast T1-weighted 3D MPRAGE images were acquired after injection of a bolus of gadobenate dimeglumine (MultiHance; Bracco Diagnostics, Princeton, New Jersey) at standard dose of 0.1 mmol/kg.

2.3. Image processing

The diffusion tensor datasets were co-registered to the b = 0 s/mm^2 images by using a 3D affine transformation estimated by maximizing the mutual information between the images. The corrected raw images were combined to estimate the DTI parametric maps by using in-house software (IDL; ITT Visual Information Solutions, Boulder, Colorado) [13]. ROIs were placed manually at three slice levels of genu, mid-body, and splenium of CC based on visual inspection by two board certified radiologists (GC and FK) (Fig. 1) [10]. FA and MD values were measured three times with different ROIs at the genu, body and splenium levels and the average values were computed. Finally FA and MD values from the genu, body and splenium were averaged and correlated with survival data.

CC invasion on conventional imaging was evaluated by a senior board-certified neuroradiologist (SM), with over 15 years of experience interpreting MRI scans of brain tumor patients. Patients were considered as having CC invasion if there were contrast-enhancing lesions on T1 weighted images or signal abnormality on T2 weighted and FLAIR images involving the CC (genu, body, or splenium) [3,14]. Patients were then divided into the following 4 groups based on CC invasion and survival time: Patients with CC invasion and short survival; Patients with CC invasion and long survival; Patients without CC invasion and short survival; Patients without CC invasion and long survival.

2.4. Statistical analysis

A non-parametric Kruskal-Wallis test was used to compare 5 groups in terms of mean MD and FA values. If there were significant difference between these groups, Mann-Whitney U test was used for pairwise comparison. A *p*-value 0.05 was considered significant. Bonferroni correction was used to adjust for multiple comparisons. Pearson correlation was performed to evaluate the relationship between FA and OS. A univariate logistic regression analysis was used to evaluate the predictive power of FA and MD for OS. Area under the curve (AUC) of receiver operating characteristic (ROC) was computed for parameters with high predictive power ($p < 0.10$, Wald test). A cutoff value for each parameter was determined by maximizing the sum of sensitivity and specificity. Kaplan-Meier survival curves were used to compare the groups with high-versus-low values in terms of OS using log-rank test. In addition, a multivariate analysis was performed including confounding variables that also affect survival such as age, gender, treatment (with or without bevacizumab therapies), KPS and tumor locations using a Cox proportional hazard ratio model. All statistical analyses were conducted by using PASW Statistics, Version 18 (IBM, New York, New York).

3. Results

The location of the tumor varied among patients including 11 frontal lobe, 12 temporal lobe, 10 parietal lobe and 3 in the occipital lobe. Additionally, 13 patients had two lobe involvements. 22 patients demonstrated CC invasion on conventional MR imaging whereas 26 patients had no CC invasion. Representative MR image from patients in these groups are shown in Fig. 2. Kruskal-Wallis test showed significant difference among the 5 groups in FA measurement ($p < 0.01$). However, there were no significant differences in MD values between these groups. Box plot of mean FA values from CC are shown in Fig. 3. The control subjects had the highest FA values (n = 17, 0.87 ± 0.03) followed by groups of long survivors without CC invasion (n = 14, 0.83 ± 0.05), long survivors with CC invasion (n = 12, 0.78 ± 0.05); short survivors without CC invasion (n = 12, 0.77 ± 0.09), and short survivors with CC invasion (n = 10, 0.64 ± 0.05). Patients with short survival and CC invasion had the lowest FA compared with other groups. P values of pairwise comparison of FA values between different groups using Mann-Whitney U test were shown in Table 1. Comparison between short survivors without CC invasion and long survivors with CC invasion, between long survivors with and without CC invasion didn't reach significant difference. There were significant differences between all other groups ($p < 0.05$). Comparison between normal subjects and other groups, between long survivors without CC invasion and short survivors with CC invasion, between short survivors with and without CC invasion still showed significant difference after Bonferroni correction ($p < 0.01$). Pearson correlation showed a moderate but significant correlation between FA and OS with r value of 0.46 ($p < 0.05$)

Univariate analysis revealed that FA had a high predictive power ($p < 0.1$, Wald test). ROC analysis indicated that a FA cutoff value of 0.70 was the best predictor for OS with an AUC of 0.77, sensitivity 1 and specificity 0.60 (Fig. 4). Kaplan-Meier survival curves demonstrated that GBM patients with high FA values (> 0.70) had a mean survival time of 20.41 ± 14.31 months whereas patients with low FA values (< 0.70) had a mean survival time of 6.79 ± 5.19 months. There was a significant difference in patients with high FA values and

low FA values ($p < 0.001$) (Fig. 5). Multivariate Cox analysis showed that KPS was related to survival ($p = 0.002$). After adjusting for age, gender, treatment, location and KPS, FA was still identified as a significant risk factor for survival (hazard ratio 0.57 for 0.1 unit increase of FA; 95% CI 0.37–0.86; $p = 0.008$).

4. Discussion

In this study, we have demonstrated that patients with CC infiltration and short survival have the lowest FA values from the CC. Also patients with low FA values from CC demonstrated shorter survival compared with those with high FA values. Our results therefore established that DTI metrics, particularly FA measurements from the CC can quantify tumor infiltration and may be used as a prognostic marker for OS in GBM patients.

Invasion of glioma cells into healthy brain tissue has been shown to occur along the white matter tracts. This occurs through a complex process of adhesion, motility, and invasion [4]. It was proposed that an interaction of tumor cells with the extracellular matrix (ECM) is mandatory to enable cell migration [15]. The invasiveness of the tumor depends on destruction of ECM components as well as on the penetration of these neoplastic cells in the adjacent normal brain structures. Glioma cells initially infiltrate or spread between and around neurons and then penetrate into the fiber tracts of white matter. Spread along white matter involves individual cells spreading within (intrafasicular), around (parafasicular) and between (interfibrillary) the axonal processes within the white matter. Little damage is caused at this stage, and the white matter remains intact. As the tumor grows and the number of tumor cells increases, the white matter is eventually destroyed by the tumor [16]. In these patients, conventional imaging can detect tumoral infiltration with presence of abnormal enhancement on post contrast T1-weighted images and associated infiltrative and expansile appearing FLAIR signal abnormality. However, in many cases, conventional imaging appears normal or there is subtle associated FLAIR signal abnormality where neoplastic infiltration cannot be differentiated from edema, gliosis, micronecrosis or local inflammatory response. Unlike conventional imaging, DTI derived FA maps can help us in not only detecting but also quantifying this “occult” tumor infiltration in the white matter. In our study, a significant decrease of FA in the CC could be secondary to reduced fiber integrity from the presence of infiltrative tumor cells, resulting in shorter survival in these patients. In contrast, patients in which FA was not as much reduced, would indicate relative preservation of fiber integrity in the CC and these patients would portend a better prognosis and overall longer survival. Besides FA, prior studies found increased MD values in the section of the CC corresponding to the tumor location [11]. However, we did not find any significant differences of MD values between groups. This may be due to the different degree of vasogenic edema in GBM.

Several factors including age, performance status, location, extent of resection, and adjuvant therapy have been reported to predict survival in GBM patients [4,17–19]. Recently, genetic markers, such as MGMT and IDH status have also been investigated as prognostic indices [20]. Previous studies reported poorer survival in patients with CC involvement, as determined by preoperative imaging [3,9,14,21]. Liang et al reported that synchronous invasion of tumor into the CC and the subventricular zone seemed to be independent factors for poor overall and progression free survival [6]. Chaichana et al demonstrated that butterfly GBM involving both cerebral hemispheres by involving and crossing the CC has poorer prognosis and that these patients may benefit from aggressive treatments including maximal debulking surgery, increasing percent resection, chemotherapy, and radiation therapy [8]. In our study, we observed that patients with higher FA values from CC survive longer compared to those with lower FA values. Our results indicate that FA values from the CC reflect the extent of tumor infiltration, which can be used as a potential prognostic marker of OS.

Our results have a potential clinical benefit and in the future may aid in individualized treatment planning because patients with low pretreatment FA values can be offered upfront alternative treatment strategies, including antiangiogenic therapy, tumor treating fields, immunotherapy, or other experimental therapies targeted toward increased survival.

Although these results are promising, this study has some limitations. The sample size is relatively small and thus the results need to be validated in a larger cohort. Also, we used hand-drawn ROIs for data analysis, which though being easy and straightforward, tends to be subjective. Different regions of CC could also be assessed separately, however, we chose to use a simplistic approach of taking an averaged ROI from the entire CC so that it can be easily performed in routine clinical workflow without requiring sophisticated image segmentation tools which may not readily available. In addition, the proximity of the CC to the tumor may also impact OS. However, measurement of proximity based on conventional imaging (FLAIR or contrast-enhanced T1images) may be challenging due to the presence of edema, inflammatory response and lack of a clear defined boundary. In order to avoid location and proximity to CC as potential confounding variables, we took an averaged FA value across the entire CC callosum. Future studies using DTI normalization, in which, the data is individually warped into a common spatial frame allowing for tract-specific analysis [22], may be needed to overcome user bias. CC invasion was determined by conventional imaging, however, we don’t have pathologic data to prove it. GBM patients in the terminal stages are referred to hospice care and it is not common practice to perform an autopsy as they already have a pathologically confirmed malignancy. Besides DTI, size of the tumor, T1/T2 ratios as well as other advanced neuroimaging techniques such as perfusion MRI and MRS will be incorporated in a future multiparametric study for better prognostication and prediction of survival in these patients

In conclusion, our results demonstrate that DTI can quantify occult tumor infiltration in the CC and serve as a sensitive prognostic marker for prediction of OS in GBM patients. However, these results need to be validated using a prospective study in a larger cohort.

Acknowledgements

We acknowledge Dr. Ruyun Jin, Medical Data Research Center, Providence Health & Services, Portland, Oregon for statistical analysis.

References

[1] M.R. Gilbert, M. Wang, K.D. Aldape, R. Stupp, M.E. Hegi, K.A. Jaeckle, T.S. Armstrong, J.S. Wefel, M. Won, D.T. Blumenthal, A. Mahajan, C.J. Schultz, S. Erridge, B. Baumert, K.I. Hopkins, T. Tzuk-Shina, P.D. Brown, A. Chakravarti, W.J. Curran Jr, M.P. Mehta, Dose-dense temozolomide for newly diagnosed glioblastoma: a randomized phase III clinical trial, J. Clin. Oncol. 31 (32) (2013) 4085–4091.

[2] J. Polivka Jr, J. Polivka, L. Holubec, T. Kubikova, V. Priban, O. Hes, K. Pivovarcikova, I. Treskova, Advances in experimental targeted therapy and immunotherapy for patients with glioblastoma multiforme, Anticancer Res. 37 (1) (2017) 21–33.

[3] K.T. Chen, T.W. Wu, C.C. Chuang, Y.H. Hsu, P.W. Hsu, Y.C. Huang, T.K. Lin, C.N. Chang, S.T. Lee, C.T. Wu, C.K. Tseng, C.C. Wang, P.C. Pai, K.C. Wei, P.Y. Chen, Corpus callosum involvement and postoperative outcomes of patients with gliomas, J. Neurooncol. 124 (2) (2015) 207–214.

[4] N.J. Mickevicius, A.B. Carle, T. Bluemel, S. Santarriaga, F. Schloemer, D. Shumate, J. Connelly, K.M. Schmainda, P.S. LaViolette, Location of brain tumor intersecting white matter tracts predicts patient prognosis, J. Neurooncol. 125 (2) (2015) 393–400.

[5] K. Kallenberg, T. Goldmann, J. Menke, H. Strik, H.C. Bock, A. Mohr, J.H. Buhk, J. Frahm, P. Dechent, M. Knauth, Abnormalities in the normal appearing white matter of the cerebral hemisphere contralateral to a malignant brain tumor detected by diffusion tensor imaging, Folia Neuropathol. 52 (3) (2014) 226–233.

[6] T.H. Liang, S.H. Kuo, C.W. Wang, W.Y. Chen, C.Y. Hsu, S.F. Lai, H.M. Tseng, S.L. You, C.M. Chen, W.Y. Tseng, Adverse prognosis and distinct progression patterns after concurrent chemoradiotherapy for glioblastoma with synchronous subventricular zone and corpus callosum invasion, Radiother. Oncol. 118 (1) (2016) 16–23.

[7] S.J. Price, A. Pena, N.G. Burnet, J.D. Pickard, J.H. Gillard, Detecting glioma

invasion of the corpus callosum using diffusion tensor imaging, Br. J. Neurosurg. 18 (4) (2004) 391–395.
[8] K.L. Chaichana, I. Jusue-Torres, A.M. Lemos, A. Gokaslan, E.E. Cabrera-Aldana, A. Ashary, A. Olivi, A. Quinones-Hinojosa, The butterfly effect on glioblastoma: is volumetric extent of resection more effective than biopsy for these tumors? J. Neurooncol. 120 (3) (2014) 625–634.
[9] K. Dziurzynski, D. Blas-Boria, D. Suki, D.P. Cahill, S.S. Prabhu, V. Puduvalli, N. Levine, Butterfly glioblastomas: a retrospective review and qualitative assessment of outcomes, J. Neurooncol. 109 (3) (2012) 555–563.
[10] B. Stieltjes, M. Schluter, B. Didinger, M.A. Weber, H.K. Hahn, P. Parzer, J. Rexilius, O. Konrad-Verse, H.O. Peitgen, M. Essig, Diffusion tensor imaging in primary brain tumors: reproducible quantitative analysis of corpus callosum infiltration and contralateral involvement using a probabilistic mixture model, NeuroImage 31 (2) (2006) 531–542.
[11] K. Kallenberg, T. Goldmann, J. Menke, H. Strik, H.C. Bock, F. Stockhammer, J.H. Buhk, J. Frahm, P. Dechent, M. Knauth, Glioma infiltration of the corpus callosum: early signs detected by DTI, J. Neurooncol. 112 (2) (2013) 217–222.
[12] U. Gimenez, A.T. Perles-Barbacaru, A. Millet, F. Appaix, M. El-Atifi, K. Pernet-Gallay, B. van der Sanden, F. Berger, H. Lahrech, Microscopic DTI accurately identifies early glioma cell migration: correlation with multimodal imaging in a new glioma stem cell model, NMR Biomed. 29 (11) (2016) 1553–1562.
[13] S. Wang, S.J. Kim, H. Poptani, J.H. Woo, S. Mohan, R. Jin, M.R. Voluck, D.M. O'Rourke, R.L. Wolf, E.R. Melhem, S. Kim, Diagnostic utility of diffusion tensor imaging in differentiating glioblastomas from brain metastases, AJNR Am. J. Neuroradiol. 35 (5) (2014) 928–934.
[14] K.J. Steltzer, K.I. Sauve, A.M. Spence, T.W. Griffin, M.S. Berger, Corpus callosum involvement as a prognostic factor for patients with high-grade astrocytoma, Int. J. Radiat. Oncol. Biol. Phys. 38 (1) (1997) 27–30.
[15] J. Zamecnik, The extracellular space and matrix of gliomas, Acta Neuropathol. 110 (5) (2005) 435–442.
[16] S.J. Price, J.H. Gillard, Imaging biomarkers of brain tumour margin and tumour invasion, Br. J. Radiol. 84 (2011) S159–67 Spec No 2.
[17] G. Coban, S. Mohan, F. Kural, S. Wang, D.M. O'Rourke, H. Poptani, Prognostic value of dynamic susceptibility contrast-enhanced and diffusion-weighted MR imaging in patients with glioblastomas, AJNR Am. J. Neuroradiol. 36 (7) (2015) 1247–1252.
[18] D. Fontaine, P. Paquis, Glioblastoma: clinical, radiological and biological prognostic factors, NeuroChirurgie 56 (6) (2010) 467–476.
[19] L.A. Mohsen, V. Shi, R. Jena, J.H. Gillard, S.J. Price, Diffusion tensor invasive phenotypes can predict progression-free survival in glioblastomas, Br. J. Neurosurg. 27 (4) (2013) 436–441.
[20] K. Wang, Y.Y. Wang, J. Ma, J.F. Wang, S.W. Li, T. Jiang, J.P. Dai, Prognostic value of MGMT promoter methylation and TP53 mutation in glioblastomas depends on IDH1 mutation, Asian Pac. J. Cancer Prev. 15 (24) (2014) 10893–10898.
[21] R. Ramakrishna, J. Barber, G. Kennedy, A. Rizvi, R. Goodkin, R.H. Winn, G.A. Ojemann, M.S. Berger, A.M. Spence, R.C. Rostomily, Imaging features of invasion and preoperative and postoperative tumor burden in previously untreated glioblastoma: correlation with survival, Surg. Neurol. Int. 1 (2010).
[22] P.A. Yushkevich, H. Zhang, T.J. Simon, J.C. Gee, Structure-specific statistical mapping of white matter tracts, NeuroImage 41 (2) (2008) 448–461.